Foundation Design for a High Bay Warehouse with a Steel Fibre Reinforced Concrete Slab

<strong/>

Kasper, T.; Sørensen, Carsten Steen; Nielsen, J. B.

Published in:
EP93 Foundations

Publication date:
2008

Document Version
Publisher's PDF, also known as Version of record

FOUNDATION DESIGN FOR A HIGH BAY WAREHOUSE WITH A STEEL FIBRE REINFORCED CONCRETE SLAB

T KASPER
COWI A/S, Parallelvej 2, 2800 Kongens Lyngby, Denmark
tkas@cowi.dk

C S SØRENSEN
COWI A/S, Parallelvej 2, 2800 Kongens Lyngby, Denmark
css@cowi.dk

J B NIELSEN
COWI A/S, Parallelvej 2, 2800 Kongens Lyngby, Denmark
jab@cowi.dk

SUMMARY: The high bay warehouse at the Carlsberg brewery in Fredericia, Denmark, is 40 m high and is founded with a 83 x 116 m foundation slab on clay till and sand layers. Due to the wind loads on the tall building, the edges of the foundation require 80 cm and 60 cm thick conventionally reinforced concrete slabs, while a 69 x 77 m and 40 cm thick steel fibre reinforced concrete (SFRC) slab forms the inner part of the foundation. Steel fibre reinforcement has been chosen mainly due to approximately 15 % lower construction costs than a comparable solution with conventional rebar reinforcement. The SFRC slab is cast in 6 panels divided by free-movement joints with shear dowels. It has to be designed for closely spaced 250 kN characteristic long-term loads for complete filling of the racks. The design has been based on a German SFRC design guideline and makes use of 3D finite element soil-structure interaction calculations applying elasto-plastic material models for both the slab and the soil.

Keywords: Finite element modelling, foundation slab, high bay warehouse, steel fibre reinforced concrete, yield line method.

INTRODUCTION

A new, fully automated high bay warehouse with computer controlled stacker cranes forms the basis for the storage logistics at the upgraded and extended Carlsberg brewery in Fredericia, Denmark. The inner part of the foundation slab of the warehouse is made

Kasper, Sørensen and Nielsen: Foundation design for a high bay warehouse with a steel fibre reinforced concrete slab. *Proceedings of the BGA International Conference on Foundations, Dundee, Scotland,24 – 27 June 2008*. IHS BRE Press, 2008.

with steel fibre reinforced concrete without rebar reinforcement (Fig. 1 and 2).

Fig. 1: *The foundation slab and the racks of the warehouse at the Carlsberg brewery during construction.*

Steel fibre reinforced concrete has been a subject of intensive research and development for a longer time [1,2]. Steel fibres can replace the conventional reinforcement in structures, for which only a little amount of rebar reinforcement would be needed. Typical fields of application are tunnel linings, pavements and floors, foundations and pipes. Steel fibres are also often used in combination with rebar reinforcement to improve the properties and the bearing capacity of concrete structures. Steel fibre reinforcement enables a simple and time-saving construction process. As a consequence, the construction costs for the inner part of the warehouse foundation were estimated to be approximately 15 % lower than with a comparable conventional reinforcement solution. In addition to the cost and construction related benefits, steel fibres introduce a favourable crack distribution behaviour and improved impact resistance of the concrete as technical benefits for this particular project. It should be noted, however, that the concrete mix design, material testing, casting technology and quality control require special care and some additional effort.

The design of the foundation slab has been based on the German SFRC design guideline [2] and is presented in detail in this paper. The bearing capacity of the slab for bending is investigated by 3D elasto-plastic soil-structure interaction calculations with a finite element program and the results are verified by comparison with solutions based on the traditional yield line method. Finite element calculations are also used for the verification of the slab deformations. Punching is investigated by simple hand calculations and the shear dowels in the joints are designed according to a formula which is based on experiments.

PROJECT BASIS

Geometry and loading

The wind loads on the 40 m high warehouse are taken by wind bracings, which are integrated into the racks in the gable areas. Between 60 and 80 cm thick conventionally reinforced concrete has therefore been used for the foundation slab in the gable areas (Fig. 2). The inner part is designed as a 40 cm thick SFRC slab without rebar reinforcement and is cast in 6 panels with 36 x 28 m maximum dimensions.

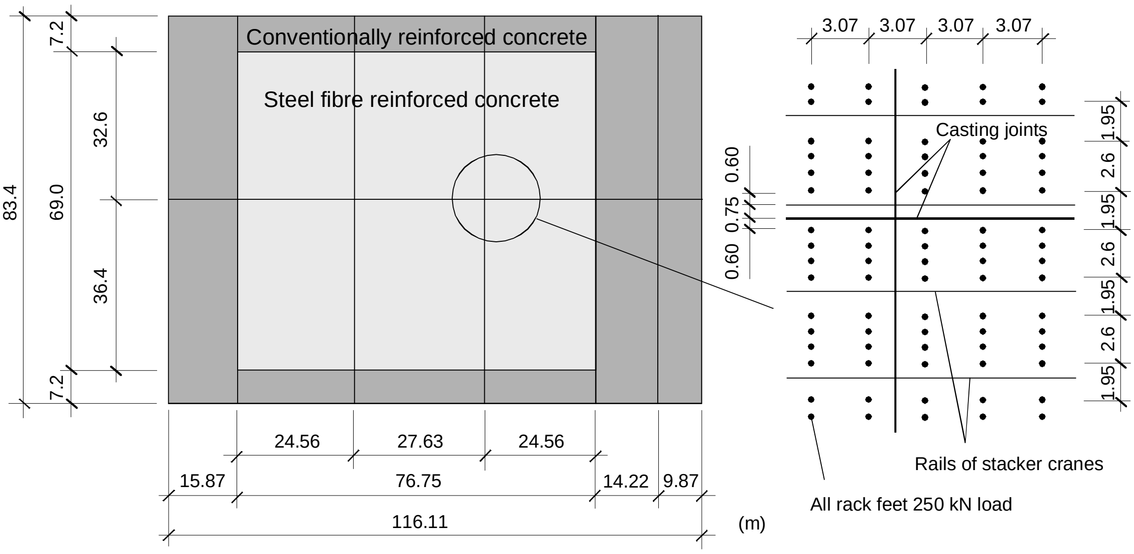

Fig. 2: *Layout and loading of the warehouse foundation.*

The loading of the SFRC slab by the racks follows a regular pattern as shown on the right hand side in Fig. 2. The characteristic foundation loads of the racks consist of 11 kN dead load, 228 kN live load (pallet weight), 3 kN snow load on the roof, 7.5 kN due to rack inclinations, 4 kN due to the stacker cranes and maximum 35 kN wind load. All racks are connected by beams in the roof. Although the major part of the wind loads is taken by the bracings in the gable areas, the deformation of the whole racking system of the warehouse due to wind causes some minor wind loads also in the racks on the SFRC slab. The warehouse is operated fully automatically by means of computer controlled stacker cranes in the aisles. The cranes have two wheels with a spacing of 5.8 m and run on rails. The maximum wheel loads are 150 kN vertical load and 280 kN horizontal breaking load.

The cohesive soil below the slab behaves stiffer and the slab therefore has a higher bearing capacity for short-term loading (i.e. undrained conditions in the soil) compared to long-term loading (i.e. drained conditions in the soil). Therefore, the slab is modelled and verified considering long-term rack loads of 11 + 228 + 3 + 7.5 + 4 = 253.5 kN ≈ 250 kN and drained conditions in the soil. Wind loads and the loads from stacker cranes are short-term loads and are not considered. The loads from the stacker cranes are distributed over a larger length by the rails and the horizontal breaking loads are considered to be uncritical for the slab.

Subsoil conditions

The subsoil consists of clay till and sand layers. The ground investigations included fifteen 12 m deep borings in a grid of 35 x 35 m and oedometer tests of soil samples. The groundwater level is located 4 m below the ground surface. The geotechnical data have been evaluated, resulting in cautious estimates of E = 40 MPa, φ' = 30º and c' = 15 kPa as input parameters for the design. The earthworks included excavation and levelling of the surface, followed by placement of 30 cm compacted sand and 20 cm compacted gravel on top. The concrete of the slab is poured on a plastic sheet which is laid on the gravel before casting.

Casting joints

Fig. 3: *Shear dowels in the casting joints.*

The casting joints are made with stretch metal and equipped with shear dowels (Fig. 3). The dowels are driven through the stretch metal into the fresh concrete during casting of the slab. They distribute the loads close to edges and corners to the neighbouring slab panel(s). In this way, they avoid the loading of free edges or free corners which may be critical for the bearing capacity, and avoid differential settlements between the slab panels. The shear dowels have a smooth surface and a plastic coating to allow shrinkage of the slab panels.

Design basis

Although design guidelines for steel fibre reinforced concrete structures have been developed in various countries, no standards exist so far. The design of the SFRC foundation slab for the warehouse has been based on a German SFRC design guideline [1].

Slab properties

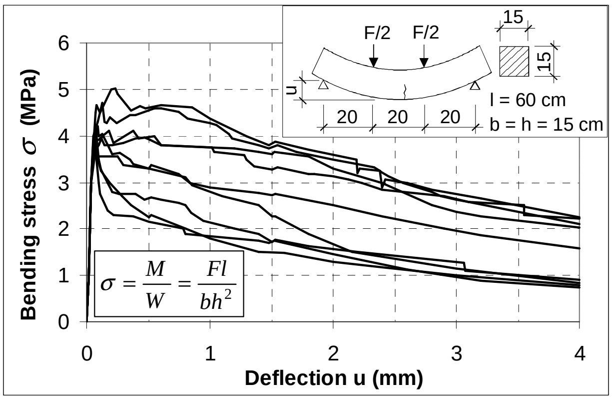

Fig. 4: *4-point beam bending test results.*

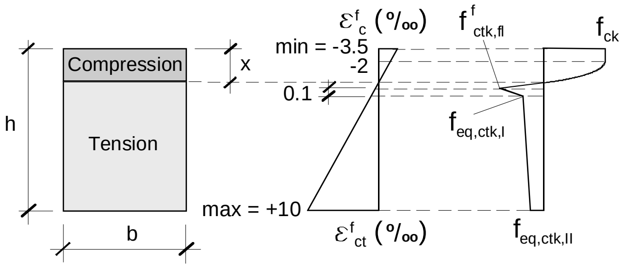

Fig. 5: *SFRC stress-strain relationship.*

The 40 cm thick slab is constructed with a C30/37 concrete and 45 kg/m^3 steel wire fibres. The fibres have a diameter of 1 mm, are 50 mm long and have hooked ends. The fibres are added to the concrete in the concrete mixer trucks at the batch plant. According to the German guideline, the strength properties of SFRC are determined from 4-point beam bending tests. The test results of 9 beams are shown in Fig. 4. The resulting strength parameters are shown in Table 1 and illustrated in Fig. 5. $f^f_{ctm,fl}$ and $f^f_{ctk,fl}$ denote the mean and characteristic tensile strength at crack initiation, $f_{eq,ctk,I}$ is the characteristic equivalent flexural tensile strength at deformation level I, i.e. shortly (0.1 ‰) after crack initiation and $f_{eq,ctk,II}$ is the characteristic equivalent flexural tensile strength at deformation level II, i.e. at large strains (10 ‰). It is interesting to note that the mean values of the equivalent flexural tensile strength parameters at deformation level I and II were found to be approximately 17 and 19 %

Table 1. *Strength parameters determined from the tests.*

Strength parameter	Value (MPa)
$f^f_{ctm,fl}$	4.160
$f^f_{ctk,fl}$	4.021
$f_{eq,ctk,I}$	1.271
$f_{eq,ctk,II}$	0.809

higher than the characteristic values. Fig. 5 illustrates the assumed stress-strain relationship of SFRC based on the German guideline for the full range of admissible compressive strains ε^f_c and tensile strains ε^f_{ct}. The design values of the strength parameters for ultimate limit state (ULS) calculations and verifications are obtained as

$$f_{cd} = f_{ck} \cdot \alpha_c^f / \gamma_c = 30 \cdot 0.85/1.5 = 17 \text{ MPa} \quad (1)$$

$$f^f_{ctd,fl} = f^f_{ctk,fl} \cdot \alpha_c^f / \gamma_{ct}^f = 4.021 \cdot 0.85/1.25 = 2.734 \text{ MPa} \quad (2)$$

$$f_{eq,ctd,I} = f_{eq,ctk,I} \cdot \alpha_c^f \cdot \alpha_{sys} / \gamma_{ct}^f = 1.271 \cdot 0.85 \cdot 0.889/1.25 = 0.768 \text{ MPa} \quad (3)$$

$$f_{eq,ctd,II} = f_{eq,ctk,II} \cdot \alpha_c^f \cdot \alpha_{sys} / \gamma_{ct}^f = 0.809 \cdot 0.85 \cdot 0.889/1.25 = 0.489 \text{ MPa} \quad (4)$$

In the above equations, α^f_c is a factor to consider long-term deterioration of concrete structures and α_{sys} is a correction factor to consider the difference in thickness between the slab and the test beams. γ_c and γ^f_{ct} are partial safety factors.

Based on Fig. 5 and considering design values of the strength parameters instead of characteristic values, it is possible to determine the evolution of the bending moment M_{ULS} with increasing deformation for the relevant situation of pure bending (normal force N = 0). Fig.6 shows the relationship between M_{ULS} and the tensile strain ε^f_{ct}.

The German guideline provides a formula for the estimation of crack widths w based on the tensile strain ε^f_{ct}, the height of the cross section h and the height of the compression zone x (cp. Fig. 5)

$$w = \varepsilon^f_{ct}(h - x) \quad (5)$$

It is important to note that the guideline requires a limitation of the crack widths in the ULS to 1/20 of the fibre length = 2.5 mm to ensure sufficient anchorage of the fibres. Fig. 7 shows the relationship between M_{ULS} and the crack width w.

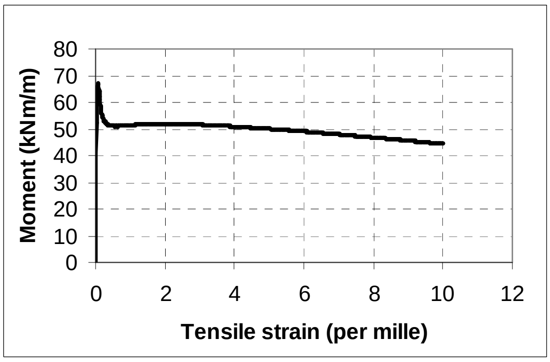

Fig. 6: *Relationship between the ULS bending moment of the slab and the tensile strain ε^f_{ct}.*

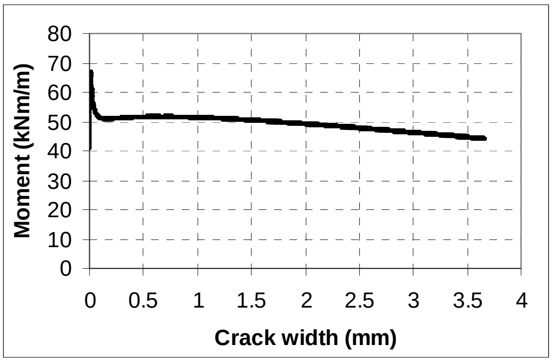

Fig. 7: *Relationship between the ULS bending moment of the slab and the crack width w.*

The ULS shear capacity of the slab has been calculated as 216 kN/m. The stiffness of a C30/37 is given in the German codes as E = 31900 MPa. A typical estimate of the Poisson's ratio is 0.17.

MODELLING AND VERIFICATION

Bearing capacity (bending)

The bearing capacity of the slab is investigated by means of 3D elasto-plastic soil-structure interaction calculations with the program Plaxis 3D Tunnel [2], complemented by comparative hand calculations based on the yield line method. One of the 3D finite element models used for the analysis of the slab is shown in Fig. 8.

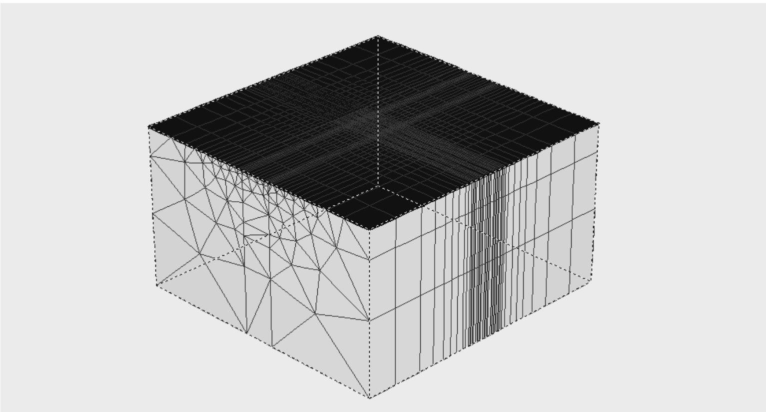

Fig. 8: *A 3D finite element model for the analysis of the foundation slab.*

It can be concluded from Figs. 6 and 7, that the bending behaviour of the slab can be modelled quite realistically as elastic-perfectly plastic, considering a plastic moment (moment capacity) of $M_{pl,ULS}$ = 45 kNm/m. This input value for the finite element calculations has been chosen conservatively based on M_{ULS} at the maximum admissible tensile strain ε^f_{ct}= 10 ‰ (Fig. 6). Based on the prescribed ULS crack width limit of max w = 2.5 mm, M_{pl} could actually be chosen slightly higher (Fig. 7).

The soil body in the models has a height of 15 m. The groundwater table is assumed 4 m below the slab. For simplification, the gravel bed and sand bed underneath the slab are not considered, which is slightly conservative as their stiffness is expected to be somewhat higher than 40 MPa. The material behaviour of the soil is described by the elasto-plastic Mohr-Coulomb model with E = 40 MPa, φ' = 30º, c' = 15 kPa and ν = 0.25, i.e. with unfactored material parameters.

The vertical boundaries of the models are fixed in the normal direction, while the bottom of the models is fixed in both horizontal directions. The displacement boundary conditions are completed by fixing the rotations around the slab edges, i.e. the vertical model boundaries are assumed to be planes of symmetry. 15-node wedge-shaped elements are used for the soil and 8-node rectangular shell elements are used to model the slab. A finer mesh is used in the loaded areas of the slab and the soil underneath to obtain reliable results.

The loads acting on top of the slab are assumed to be dispersed through the slab to the neutral axis with a spread-to-depth ratio of 1:1. Hence, the loads transferred by the 16 x 18 cm baseplates at the rack feet are modelled as uniformly distributed loads on the slab elements over areas of 56 x 58 cm.

The casting joints with shear dowels are considered in the models by means of narrow strips of elements with a small plastic moment corresponding to the bending capacity of the steel dowels of M_{pl} = 1.1 kNm/m.

The ultimate load levels are determined by a stepwise increase of the loads on the slab and an evaluation of the corresponding crack widths. It should be noted that the elasto-plastic finite element calculations represent a smeared crack modelling approach and that the German guideline is also based on a stress-strain relationship. For a given load level, the calculated deformations of the slab are inspected. By taking the displacements of three adjacent nodes around the location and in the direction of maximum bending curvature of the slab, a second-order polynomial $u = ax^2 + bx + c$ can be determined which matches the displacement profile. This approach is consistent with the finite elements used in the calculations, which also have a second-order approximation of displacements. From the curvature, which is the second derivative of the displacements $\kappa = u'' = a$, the strain difference over the height of the cross section can be determined as $\Delta\varepsilon = \varepsilon^f_{ct} - \varepsilon^f_c = \kappa \cdot h$. $\Delta\varepsilon$ can now be used together with the condition $N = 0$ (pure bending) to determine the crack width based on Fig. 5 and Eq. (5). The ultimate load level is reached when the calculated crack width reaches the prescribed limit of 2.5 mm. The German guideline requires a partial safety factor on the loads of 1.5, i.e. the predicted ultimate load level should be at least 1.5 x 250 = 375 kN.

In order to find the critical loading situation for the bearing capacity of the slab, different cases have been investigated. The results for case 1 - a single load far from joints - is shown in Fig. 9. The influence of the joints is checked by the analysis of case 2 - a single load close to joints - as shown in Fig. 10.

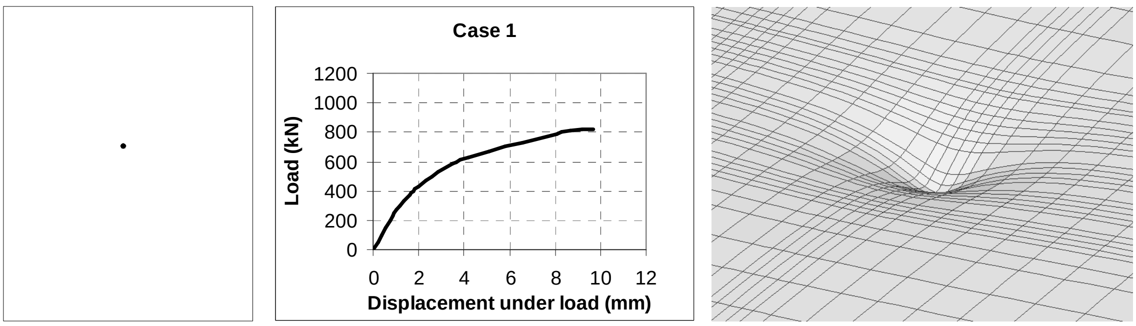

Fig. 9: *Case 1 - a single load far from joints. Layout, load-displacement curve and magnified displacements. The predicted ultimate load level is 821 kN.*

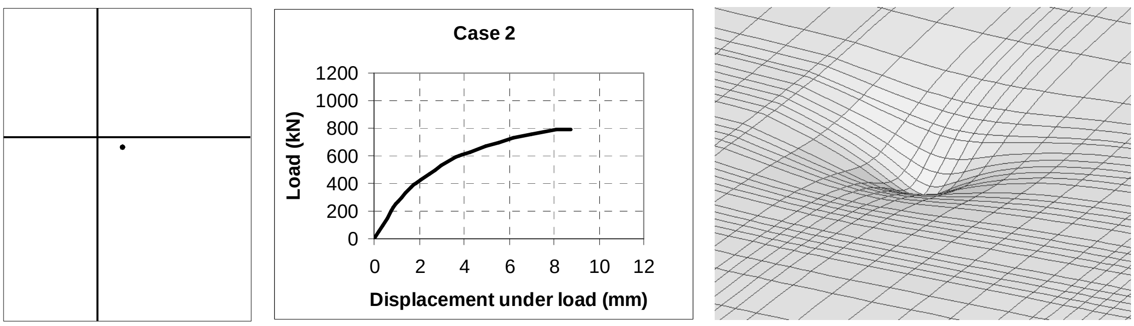

Fig. 10: *Case 2 - a single load close to joints. Layout, load-displacement curve and magnified displacements. The predicted ultimate load level is 791 kN.*

It is found that the difference in the ultimate load levels between case 1 and 2 is quite small. This is due to the minimum distance of the loads from the joints of 60 cm and due to the load transfer between the slab panels by the shear dowels in the joints. Nevertheless, the ultimate load level is smaller and therefore, case 3 - 8 loads close to joints - and case 4 - full loading of the slab - are analysed considering the joints.

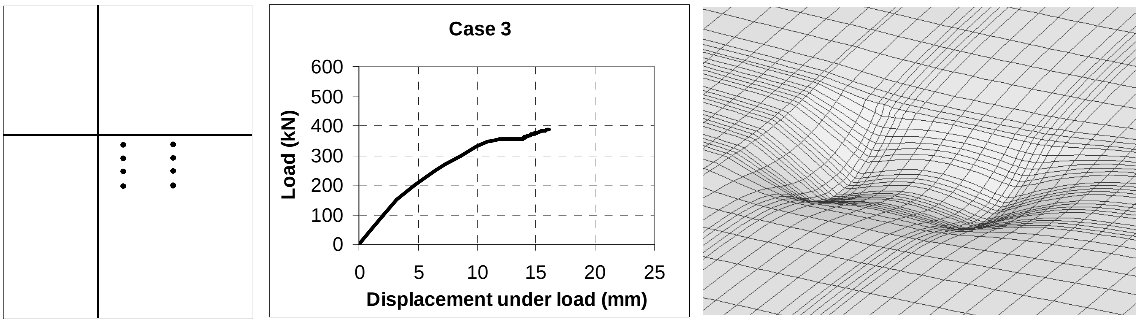

Fig. 11: *Case 3 - 8 loads close to joints. Layout, load-displacement curve and magnified displacements. The predicted failure load level is 390 kN.*

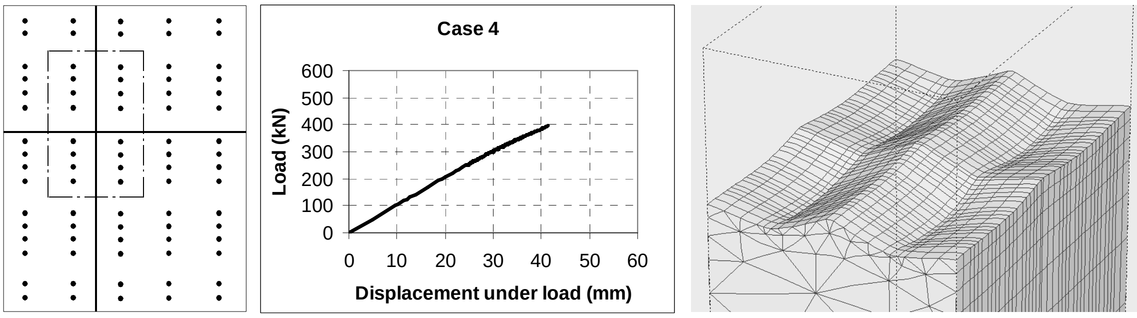

Fig. 12: *Case 4 - Full loading of the slab. Layout, load-displacement curve and magnified displacements. The predicted ultimate load level is 388 kN.*

The results of case 3 and 4 confirm the expectation that the ultimate load level decreases with increasing number of loads. Case 4 with full loading of the slab yields the lowest ultimate load level. For single loads, the ultimate load level is clearly reached before crack widths and fibre anchorage become critical (cp. the load-displacement curves in Fig. 9 and 10). With increasing number of loads (Fig. 11 and 12), failure of the slab seems to be more and more governed by the crack width criterion, i.e. fibre anchorage.

Analytical solutions for case 1 and 4 can be derived based on the yield line method [3,4] as shown in Fig. 13. The yield line method is based on the assumption of rigid-plastic behaviour of a slab with distinct yield lines (cracks) at failure. Based on

- a chosen, kinematically possible yield line (crack) pattern
- a suitably chosen distribution of soil stresses and
- a corresponding virtual displacement field (rotations φ),

an equilibrium relation between the moment capacities of the slab in the yield lines (cracks) and the loads on the slab can be derived from the principle of virtual work.

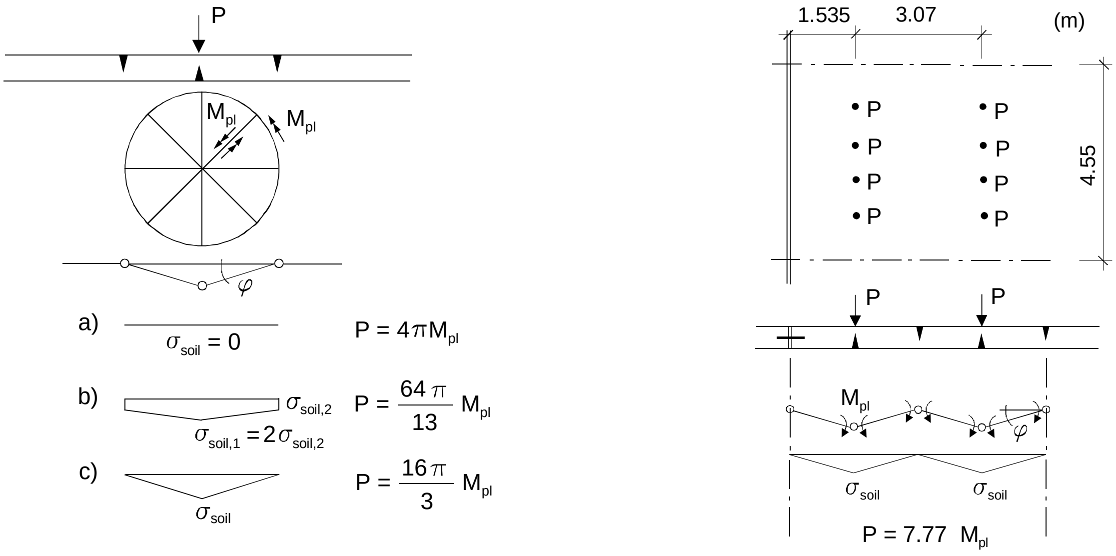

Fig. 13: *Solutions for the ultimate load level in case 1 (left) and 4 (right) based on the yield line method.*

In the finite element calculations for case 1, the distribution of the vertical soil stresses under the slab at ultimate load level has been found to be close to assumption c) in Fig. 13 (left). The ultimate load levels predicted by the finite element calculations of 821 kN for case 1 and 388 kN for case 4 are about 10 % higher than the corresponding yield line solutions of 753 kN for case 1 c) and 350 kN for case 4. Considering the basic differences in the two approaches, this result is quite satisfying. The lowest ultimate load level of 388 kN predicted by the FE calculation is slightly above the requirement (1.5 x 250 = 375 kN), while the yield line solution of 350 kN is slightly below the requirement. It could be argued that rather the 17 to 19 % higher mean values of the equivalent flexural tensile strength parameters than the characteristic values are decisive for failure modes involving longer cracks. Thus, considering the different conservative assumptions in terms of soil stiffness and moment capacity of the slab, the calculated safety level is acceptable.

Shrinkage stresses have not been considered, since they are generally small close to edges and corners of slab panels. Furthermore, they can be neglected if they are released (distributed) over a larger number of cracks as in the critical case 4. Case 1 and 2 are uncritical and case 3 with considered load differences between neighbour racks of 100 / 0 % is very unlikely.

Shear capacity (punching)

The shear capacity of the SFRC slab is 216 kN/m. Punching is verified in a perimeter distance of 1.5 times the height of the cross section (1.5 x 0.4 = 0.6 m) from the loaded area. The verification for a single rack load and a row of 4 rack loads by a simple, conservative hand calculation without consideration of the soil support is shown in Fig. 14. It is found that punching is not a problem.

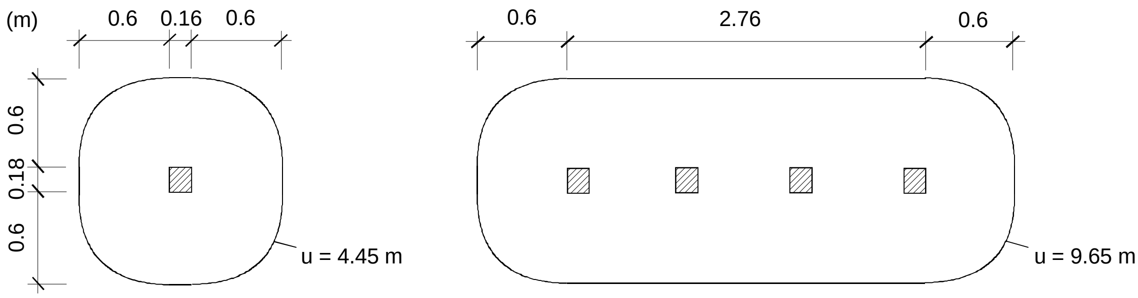

$$v_{ED} = \frac{250 \cdot 1.5}{4.45} = 84 \text{ kN/m} < v_{RD} = 216 \text{ kN/m OK} \qquad v_{ED} = \frac{4 \cdot 250 \cdot 1.5}{9.65} = 155 \text{ kN/m} < v_{RD} = 216 \text{ kN/m OK}$$

Fig. 14: *Verification of punching of the slab.*

Deformation limitations (SLS)

The racking system supplier required a limitation of the deformation induced slab inclinations in the serviceability limit state (SLS) to $5 \cdot 10^{-4}$. This corresponds to differential slab settlements of 5 mm in 10 metres or a corresponding horizontal rack displacement of 20 mm in 40 m height. The reason for the strict requirement is to ensure precision and thus optimal performance of the stacker cranes.

This requirement is verified by an elastic calculation. First, the expected long-term average load level of 80 % in the warehouse is considered by applying a uniform load level of 0.8 x 250 = 200 kN in a drained calculation step. Afterwards, short-term load differences are considered by a stepwise increase of the loads in one area to 100 % and a simultaneous decrease of the loads in the neighbouring areas to 60 % assuming undrained conditions. Fig. 15 (left) illustrates the investigated scenario. The corresponding slab displacements are illustrated in Fig. 15 (right). The maximum slab inclination reaches $5 \cdot 10^{-4}$ at approximately 32 % load difference. It is unlikely that such a load difference will be reached or exceeded.

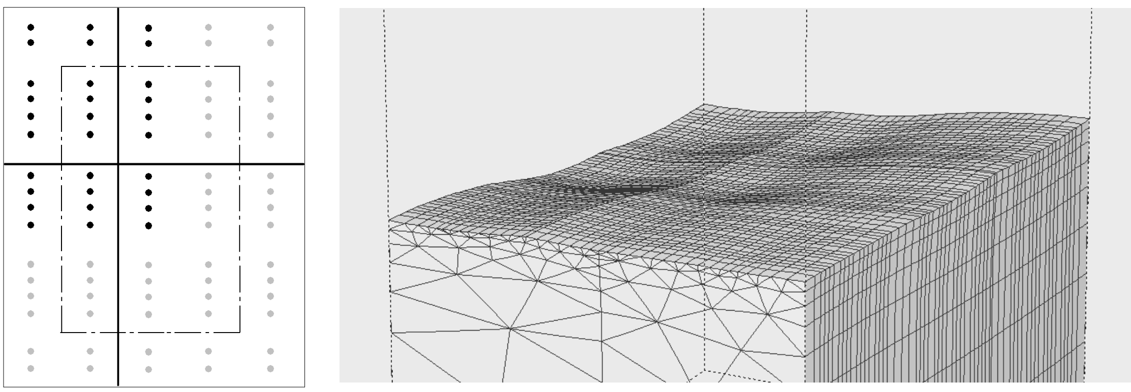

Fig. 15: *Analysis of short-term load differences between neighbour racks. Layout (black dots: from 80 % to 100 % rack load, grey dots: from 80 % to 60 % rack load) and magnified displacement plot.*

The maximum bending moments in the slab for 100 % load level are approximately 80 kNm/m, corresponding to a flexural tensile stress of $\sigma = M/W = 3.0$ MPa. Shrinkage stresses in the slab can be estimated with an empirical formula

$$\sigma = \frac{0.5 \cdot c \cdot L \cdot G}{h} \tag{6}$$

where c denotes the friction parameter soil-concrete, L is the distance between joints, G is the slab weight and h is the slab height. Based on c = 1 (full friction), max L = 36 m, G = 9.6 kN/m^2 and h = 0.4 m, the shrinkages stresses are expected to be 0.43 MPa. Comparing the maximum flexural tensile stress, shrinkage stress and flexural tensile strength 3.0 + 0.43 < $f^f_{ctk,fl}$ = 4.021 MPa, it is concluded that cracking of the slab under service load is unlikely. According to Fig. 9 to 12 there is a smooth stiffness degradation after the onset of plastic deformations (cracking), i.e. the elastic stiffness would still be a good approximation even for load levels slightly above the cracking load level. Therefore, an elastic calculation has been suitable for the verification of slab inclinations.

Shear dowels

The maximum shear forces in the joints have been found in case 3 (120 kN/m at load level 250 kN). The dowels have been designed using the formula [5]

$$F_u = 250\, d_s \sqrt{f_{yk}\ f_{c,cube}} \tag{7}$$

which is based on experiments. In this formula, F_u (N) denotes the shear capacity of the dowel, d_s (cm) is the dowel diameter, f_{yk} (MPa) is the yield strength of the dowel material and $f_{c,cube}$ (MPa) is the compressive cube strength of the concrete. Using 50 cm long steel dowels with a diameter of 2.5 cm, a yield strength f_{yk} = 240 MPa and a dowel spacing of 25 cm, a safety factor of 5 is achieved, which is recommended to limit the dowel displacement to 0.005 d_s = 0.125 mm.

CONCLUSIONS

The combination of conventionally reinforced concrete to take the wind loads from the bracings in the gable areas and steel fibre reinforced concrete in the inner part had been chosen as an optimised solution for the foundation slab of the high bay warehouse. Based on flexural strength parameters derived from beam bending tests, it has been found that the bending behaviour of the SFRC slab can be adequately described as elastic-perfectly plastic. Motivated by this fact, the bearing capacity of the slab has been verified by 3D finite element calculations, in which both the slab and the soil are modelled as elasto-plastic and in which the soil-structure interaction is appropriately considered. The calculated stress distributions in the soil and deformation patterns of the slab have been used as input for comparative calculations based on traditional yield line theory. The results of both methods show satisfying agreement. The FE calculations provided a consistent approach not only to study and verify the bearing capacity for different loading situations, but also to verify the slab deformations and to determine the relevant shear forces for the design of the shear dowels in the joints. Punching of the slab was verified by simple hand calculations.

ACKNOWLEDGEMENTS

The authors gratefully acknowledge the permission from Carlsberg Denmark A/S brewery to publish this paper.

REFERENCES

1. Maidl B. *Steel fibre reinforced concrete*. Ernst & Sohn, 1995.
2. Gossla U. *Tragverhalten und Sicherheit betonstahlbewehrter Stahlfaserbeton-bauteile (Load Bearing Behaviour and Safety of Steel Fibre Concrete with Additional Reinforcing Bars)*. DAfStb Heft 501. Beuth, Berlin, 2000.
3. Deutscher Beton- und Bautechnik-Verein (DBV). *Merkblatt Stahlfaserbeton*. October, 2001.
4. Plaxis b.v., Netherlands: Plaxis 3D Tunnel. *www.plaxis.nl*.
5. Johansen K W. *Yield-line-theory*. Cement and Concrete Association, London, 1962.
6. Meyerhof G G. Load carrying capacity of concrete pavements. *Journal of the Soil Mechanics and Foundations Division*, Vol. 88, June 1962, pp 89–166.
7. Leonhardt F. *Vorlesungen über Massivbau*. Springer, 1986.